

Species difference in intestinal absorption mechanism of etoposide and digoxin between cynomolgus monkey and rat

メタデータ	言語: eng 出版者: 公開日: 2017-10-03 キーワード (Ja): キーワード (En): 作成者: メールアドレス: 所属:
URL	http://hdl.handle.net/2297/12346

Species difference in intestinal absorption mechanism of etoposide and digoxin
between cynomolgus monkey and rat

Nishimura T¹, Kato Y¹, Amano N², Ono M², Kubo Y¹, Kimura Y², Fujita H² and
Tsuji A¹.

Affiliations

1) Division of Pharmaceutical Sciences, Graduate School of Natural Science and
Technology, Kanazawa University, Kakuma-machi, Kanazawa 920-1192, Japan

2) Discovery Research Center, Pharmaceutical Research Division, Takeda
Pharmaceutical Co. Ltd, Osaka 532-8686, Japan

Address correspondence to:

Akira Tsuji, Ph. D., Professor

Graduate School of Natural Science and Technology,

Kanazawa University,

Kakuma-machi, Kanazawa 920-1192, Japan

TEL: +81-76-234-4479

FAX: +81-76-264-6284

E-mail: tsuji@kenroku.kanazawa-u.ac.jp

Running Title

Species difference in intestinal absorption of etoposide

Abbreviations

AP-to-BL, apical to basolateral; AUC, area under the concentration curve; CYP, cytochrome P450; FD-4, FITC-dextran (mw. 4000); P-gp, P-glycoprotein; LC/MS/MS, liquid chromatography coupled with tandem mass spectrometry; SLC, solute carrier.

Key words

Intestinal absorption; bioavailability; species difference; cynomolgus monkey; P-glycoprotein

Submitting to *Pharmaceutical Research*

Number of total pages of the manuscript:

Number of Figures: 4

Number of Tables: 2

Number of words in abstract: 198

Abstract

Purpose. The oral bioavailability of some therapeutic agents is markedly lower in cynomolgus monkeys than in humans. We investigated small-intestinal absorption of the P-glycoprotein (P-gp) substrates etoposide and digoxin in monkeys to clarify the influence of efflux transport on their intestinal permeability.

Methods. The pharmacokinetics of etoposide and digoxin was examined in monkeys and rats after oral and intravenous administration. Intestinal permeability and segmental differences in permeability were investigated with an Ussing-type chamber.

Results. The bioavailability of etoposide was 12.9 and 13.9% in monkeys and rats, respectively. Total body clearance of etoposide in monkeys was much less than hepatic blood flow, suggesting that the bioavailability would be limited at intestinal absorption. Marked vectorial transport of etoposide in the secretory direction was observed in rats, especially in the lower small intestine, and segmental differences were consistent with the distribution of P-gp expression. Vectorial transport was minimal in monkey small intestine. Our kinetic analysis indicated that P-gp contributes little to the intestinal permeability of etoposide and digoxin in monkeys, and apical uptake is rate-limiting.

Conclusion. Low bioavailability of etoposide in monkeys is due to poor intestinal uptake resulting from low influx from the apical side, rather than secretion via P-gp.

Introduction

Absolute oral bioavailability is an important determinant of the pharmacological efficacy of orally administered drugs. However, it is difficult to predict oral bioavailability in humans from preclinical studies, even using non-human primates. For example, cynomolgus monkeys are sometimes used in preclinical studies, but they tend to exhibit lower bioavailability than humans (1-3). In extreme cases, this may result in inappropriate termination of drug development. It is therefore important to understand in detail the processes involved in small intestinal absorption in monkeys.

Recently, we investigated the oral bioavailability and intestinal absorption mechanism of midazolam, a typical substrate of CYP3A, in both monkeys and rats. While the oral bioavailability of midazolam was poor in both species, the intestinal availability of midazolam was poor only in monkeys (4). We found that potent metabolic activity for midazolam was asymmetrically localized inside the small-intestinal cells in monkey, suggesting that midazolam would be rapidly and extensively metabolized after having been taken up across the apical membrane (4). However, it remains to be addressed whether poor bioavailability of other drugs in monkeys can be similarly explained, since penetration of xenobiotics across the small intestine is influenced at least two factors, i.e., CYP3A and P-gp, the substrate specificities of which partially overlap (5, 6). Accordingly, the species difference of bioavailability of at least some drugs might not be due to a difference in intestinal metabolism, but rather to a difference of efflux transport across small intestinal epithelial cells.

Several efflux pumps, such as P-gp, multidrug resistance-associated protein 2 (ABCC2) and breast cancer resistance protein (ABCG2), are expressed on the apical membrane of intestinal epithelial cells, and are involved in efflux of substrates from inside the cells into the intestinal lumen (7-10). P-gp is a well-known efflux pump that limits the intestinal penetration of many xenobiotics, including various drugs (11, 12). However, little is known about the contribution of these efflux transporters to intestinal drug absorption in cynomolgus monkeys.

To address whether the lower oral bioavailability depends on membrane permeability in the small intestinal tissues, it is necessary to study the

intestinal absorption mechanism using a model drug that shows poor bioavailability in monkeys. In the present study, we selected two test compounds (etoposide and digoxin) to assess the involvement of P-gp in intestinal absorption in monkeys, based on the following criteria: a) substrates of P-gp, b) sufficient oral bioavailability at least in humans, c) poor metabolic clearance with oral bioavailability being primarily determined by the intestinal first-pass removal. Etoposide, a topoisomerase II inhibitor, is a P-gp substrate, and its intestinal absorption is regulated by P-gp (13, 14). Plasma clearance of etoposide is 0.68 (mL/min/kg), and its oral bioavailability is 52% in humans (15). Therefore, etoposide should be a suitable probe for studying the effect of P-gp on intestinal drug absorption, since its membrane permeability in the small intestine directly affects its oral bioavailability. Digoxin, another typical substrate of P-gp, was also used in the present study to analyze the influence of P-gp on intestinal absorption in monkeys, since hepatic first-pass removal of digoxin is not large. With these drugs, the bioavailabilities of which are primarily determined by the small intestinal permeability, we expected that it would be possible to assess the contributions of apical uptake and efflux processes in the small intestine to the overall bioavailability. For comparison, we also investigated theophylline, which is rapidly absorbed with minimal first-pass metabolism, and is poorly transported by P-gp.

In the present study, we used an Ussing-type chamber system, since its advantages as an experimental system for analyzing intestinal drug transport include easy assessment of vectorial transport across intestinal tissues, and the ability to determine kinetic parameters of permeation across the apical and basal sides, so that the rate-limiting process in the overall intestinal permeability can be identified.

Materials and Methods

Chemicals.

Etoposide, digoxin and FD-4 were purchased from Sigma (St. Louis, MO). Theophylline was purchased from Wako Pure Chemical Industries, Ltd. (Osaka, Japan). [³H]Digoxin (0.33 TBq/mmol) was purchased from PerkinElmer Life and Analytical Sciences (Boston, MA). [¹⁴C]Inulin (161 MBq/g) was purchased from ICN Biomedicals, Inc. (Costa Mesa, CA). C219 monoclonal antibody (Dako, Carpinteria, CA) and anti-mouse IgG (Amersham Biosciences, Buckinghamshire, UK) were commercial products. All other chemicals were commercial products of reagent grade.

Animals

Cynomolgus monkeys (5-6 years old, male) were purchased from China National Scientific Instruments & Materials Import / Export Corporation (China), and maintained on approximately 108 g of food (Teklad Global 25% Protein Primate Diet, Harlan Teklad, Madison, WI) once a day, with free access to water. Sprague-Dawley rats (7 weeks old, male) were purchased from Japan SLC (Hamamatsu, Japan) and maintained with free access to food and water. Animals were deprived of food for one day before experiments. Animal studies were performed in accordance with the Guidelines for the Care and Use of Laboratory Animals, Kanazawa University.

Pharmacokinetic properties of etoposide, digoxin and theophylline in monkeys and rats

Etoposide, digoxin and theophylline were each dissolved in a mixture of dimethylacetamide and saline (1:1, v/v) for intravenous bolus injection at a dose of 0.1 mg/0.2 mL/kg for monkeys and 0.1 mg/mL/kg for rats. Intravenous bolus injection was conducted without cannulation into the saphenous vein in monkeys and into the femoral vein in rats. Etoposide and theophylline were suspended in 0.5% methylcellulose solution for oral administration at a dose of 1 mg/2 mL/kg for monkeys and 1 mg/5 mL/kg for rats. Digoxin was suspended in 0.5% methylcellulose solution for oral administration at a dose of 0.3 mg/2 mL/kg for monkeys. Oral administration to rats was done by gavage. Blood samples were

collected at 5, 10, 15, and 30 min, and 1, 2, 4, 8, and 24 hr after intravenous administration and at 15 and 30 min, and 1, 2, 4, 8, and 24 hr after oral administration in monkeys and rats.

Transport experiment and measurement of radioactivity in Ussing-type chamber

The apparatus and the method for the preparation of monkey and rat small intestinal tissue were described previously (4). Briefly, segments of upper, middle and lower small intestine isolated from monkeys and rats were used for the Ussing-type chamber study. Isolated intestinal tissue sheets from which the muscle layer had been removed with fine tweezers were mounted vertically in Ussing-type chambers that provided an exposed area of 0.75 cm² for monkeys and 0.25 cm² for rats. The volume of bathing solution on each side was 1.2 mL, and the solution temperature was maintained at 37 °C in a water-jacketed reservoir. The test solution was composed of (mM): 128 NaCl, 5.1 KCl, 1.4 CaCl₂, 1.3 MgSO₄, 21 NaHCO₃, 1.3 KH₂PO₄, 10 NaH₂PO₄ and 5 D-glucose (adjusted to pH 6.0 or 7.4 for the apical (AP) or basal (BL) side, respectively), and gassed with 95% O₂/5% CO₂ before and during the transport experiment. The etoposide or digoxin concentration on the donor side was set to be 30 μM and the theophylline concentration was set to be 300 μM. At 5, 30, 60, 90 and 120 min, a 250-μL aliquot of acceptor-side buffer was sampled and replaced with an equal volume of fresh buffer. The experiment was continued for 120 min, after which time the tissue and buffer on the donor side were also collected. [³H]Digoxin in 250-μL aliquots of the apical and basal side buffer solution from the rat Ussing-type chamber was directly mixed with 3 mL of scintillation cocktail (Clearsol-I, Nacalai tesque, Kyoto, Japan). Rat intestinal tissue homogenates were solubilized with 1 mL of Soluene 350 (Packard BioScience B.V., Groningen, Netherlands) for 3-4 hr at 55 °C, and then 100 μL of H₂O₂ was added and neutralized with 100 μL of 5 N HCl. Radioactivity was measured with a liquid scintillation counter (LSC-5100, Aloka Co., Ltd., Tokyo, Japan).

Serum protein binding of etoposide

The free fraction of etoposide in serum was determined *in vitro* by equilibrium

dialysis methods using 96-well Equilibrium DIALYZER (molecular weight cut-off of 10 kDa, Harvard Bioscience, Holliston, MA). Etoposide was added to monkey and rat serum at a concentration of 1 μ M. Phosphate-buffered saline (PBS) was used as dialysis buffer. Dialysis was conducted in quadruplicate for 20 hr at room temperature. Concentrations of compounds in dialysate were analyzed by LC/MS/MS.

Measurement of drug concentration by means of high-performance liquid chromatography with tandem mass spectrometry (LC/MS/MS)

Etoposide, digoxin or theophylline in 100- μ L aliquots of plasma, the apical-side and basal-side buffers from the Ussing-type chamber, and tissue homogenates were extracted with 10 μ L of acetonitrile and 100 μ L of internal standard solution (100 ng/mL alprenolol, 50 ng/mL lanatoside C or 100 ng/mL phenytoin, respectively, in acetonitrile). The mixtures were centrifuged at 3,000 rpm to remove precipitated protein. For etoposide, 100 μ L of supernatant was then diluted with 200 μ L of 0.01 M ammonium formate (pH 3.0). A 20- μ L aliquot was analyzed by means of LC/MS/MS. The flow rate was set at 0.2 mL/min. Separation was performed at 40 °C with a gradient system generated from 0.01 M ammonium formate, pH 3.0 (A) and 0.2% formic acid in acetonitrile (B): B was held at 10% for 1 min, increased linearly to 90% in 1 min, held at 90% for another 2.5 min, and then brought back to 10% in 0.1 min, followed by re-equilibration for 2.9 min.

For determination of digoxin in rat plasma, 100 μ L of supernatant was diluted with 100 μ L of 0.01 M ammonium formate (pH 3.0). For digoxin in monkey plasma, 150 μ L of supernatant was evaporated and the residue was suspended in 50 μ L of a mixture of 0.01 M ammonium formate and acetonitrile (3:1). Each solution was centrifuged at 15,000 rpm for 5 min. For digoxin in monkey intestinal tissue, 150 μ L of supernatant was diluted with an equivalent volume of 0.01 M ammonium acetate. A 20- μ L aliquot was then analyzed by means of LC/MS/MS. The flow rate was set at 0.2 mL/min, and the eluent consisted of 0.02 M ammonium formate (0.02 mL/min) and the following gradient system (0.18 mL/min). Separation was performed at 40 °C with the gradient system generated from distilled water (A) and acetonitrile (B): B was held at 15% for 1

min, increased linearly to 90% in 1.5 min, held at 90% for another 2 min, and then brought back to 15% in 0.1 min, followed by re-equilibration for 1.9 min. For determination of theophylline, 100 μ L of supernatant was diluted with 200 μ L of 0.01 M ammonium formate (pH 3.0). A 20- μ L aliquot was taken and analyzed by means of LC/MS/MS. The flow rate was set at 0.2 mL/min. Separation was performed at 40 °C with a gradient system generated from 0.01 M ammonium formate, pH 3.0 (A) and methanol (B): B was held at 15% for 0.75 min, increased linearly to 90% in 0.25 min, held at 90% for another 4.5 min, and then brought back to 10% in 0.1 min, followed by re-equilibration for 3.4 min. The LC system was a Shimadzu series SIL-10AHC (Shimadzu, Kyoto, Japan). The analytical column was a CAPCELL PAK C18 MGII (2.0 x 20 mm for etoposide and digoxin), and CAPCELLPAK C8 (2.0 x 150 mm for theophylline) column (Shiseido, Tokyo, Japan). Mass spectrometry experiments were conducted on a PE-Sciex API-3000 or API-4000 instrument (Applied Biosystems, Foster City, CA) with positive (for etoposide and digoxin) or negative (for theophylline) ionization electrospray. The multiple reaction monitor was set at 589.1 to 229.0, 249.9 to 116.3, 798.7 to 651.2, 1002.5 to 651.2, 179.0 to 163.9 and 250.8 to 101.8 m/z for etoposide, alprenolol, digoxin, lanatoside C, theophylline and phenytoin, respectively.

Western blot analysis

The tissue preparation of monkey and rat intestinal mucosa was described previously (4). All samples were diluted to equal protein concentration (4.4 mg protein/mL), and then 43.4 mM Tris-HCl, pH 6.8, 1% SDS, 5% β -mercaptoethanol (final concentrations) and urea were added. Proteins (20 μ g/lane) were separated by SDS-PAGE (10% polyacrylamide gel), and transferred onto a polyvinylidene difluoride membrane (Millipore Corporation, Billerica, MA) at 2 mA/cm² for 120 min. Ponceau S staining confirmed that each lane was equally well transferred to the membrane (data not shown). For detection of monkey P-gp protein, the membrane was incubated in Tris-buffered saline (20 mM Tris-HCl, pH 7.5 and 137 mM NaCl, 0.1% Tween 20) containing 5% skim milk for blocking, and then incubated with 1% C219 monoclonal antibody (DAKO) in the above buffer containing 0.5% skim milk. The

membranes were rinsed with Tris-buffered saline containing 0.1% Tween 20, and reacted with 0.05% horseradish peroxidase-conjugated donkey anti-mouse IgG as the secondary antibody (GE Healthcare). Bands were visualized by using the enhanced chemiluminescence detection method with the ECL Plus Western blotting detection system (GE Healthcare). Quantitative analysis was done by densitometry using a light-capture apparatus (AE6961FC, ATTO Bioscience, Tokyo, Japan).

Data analysis

Transport clearances in the Ussing-type chamber were estimated by means of the following equations:

For AP-to-BL transport,

$$CL_{\text{abs}} = \frac{X_{\text{basal}}}{AUC_{\text{apical}}} \quad (1)$$

For BL-to-AP transport,

$$CL_{\text{sec}} = \frac{X_{\text{apical}}}{AUC_{\text{basal}}} \quad (2)$$

where CL_{abs} , X_{basal} and AUC_{apical} mean transport clearance in the AP-to-BL direction, the amount of parent drug that appeared in the BL compartment, and the area under the parent drug concentration curve in the AP compartment, respectively, while CL_{sec} , X_{apical} and AUC_{basal} are the corresponding parameters in the opposite direction. Both CL_{abs} and CL_{sec} were measured by assuming that drug concentration in the tissue and drug appearance in the acceptor side reached at the steady-state. Membrane permeability was analyzed was calculated by use of the following equations:

$$CL_{\text{abs}} = CL_{\text{AT}} \times \frac{CL_{\text{TB}}}{CL_{\text{TA}} + CL_{\text{TB}}} \quad (3)$$

$$CL_{\text{sec}} = CL_{\text{BT}} \times \frac{CL_{\text{TA}}}{CL_{\text{TA}} + CL_{\text{TB}}} \quad (4)$$

CL_{AT} is defined as the membrane permeability across the apical membrane from outside of the tissue to inside of the tissue (apical-to-tissue). Similarly, CL_{TA} , CL_{TB} and CL_{BT} represent the tissue-to-apical, tissue-to-basal, and basal-to-tissue membrane permeabilities, respectively.

If we assume a steady-state condition for the amount of parent drug in tissue and a sink condition for the acceptor, the influx rate from the donor-side chamber into tissue is equal to the elimination rate from tissue.

For AP-to-BL transport,

$$CL_{AT} \times C_{apical} = (CL_{TA} + CL_{TB}) \times C_{tissue, a - b} \quad (5)$$

For BL-to-AP transport,

$$CL_{TB} \times C_{basal} = (CL_{TA} + CL_{TB}) \times C_{tissue, b - a} \quad (6)$$

where $C_{tissue, a-b}$ and $C_{tissue, b-a}$ are the parent drug concentration in small intestinal tissue, calculated on the assumption that specific gravity of the tissue is unity, at the end of the experiment after drug addition to the apical-side and basal-side chambers, respectively. Therefore, all the microscopic parameters ($CL_{AT} \sim CL_{BT}$) can be directly calculated by use of the following equations:

$$CL_{AT} = CL_{abs} \times (CL_{TA} + CL_{TB}) / CL_{TB} \quad (7)$$

$$CL_{TA} = CL_{sec} / (C_{tissue, b - a} / C_{basal}) \quad (8)$$

$$CL_{TB} = CL_{abs} / (C_{tissue, a - b} / C_{apical}) \quad (9)$$

$$CL_{BT} = CL_{sec} \times (CL_{TA} + CL_{TB}) / CL_{TA} \quad (10)$$

Statistical Analysis

Plasma concentrations of drugs and pharmacokinetic parameters in vivo are presented as mean \pm standard deviation (S.D.). Other data are presented as mean \pm standard error of the mean (S.E.M.). Statistical comparisons were performed by means of Student's *t*-test or ANOVA with Tukey's post hoc comparison test. Values of $p < 0.05$ were considered to be significant. Experimental numbers refer to the numbers of animals.

Results

Oral absorption of model drugs *in vivo*

To evaluate the disposition of etoposide, digoxin and theophylline in monkeys, we measured pharmacokinetic parameters after intravenous and oral dosing (Fig. 1 and Table 1). Theophylline was almost completely absorbed with 90-100% bioavailability (B.A.) in monkeys and rats (Table 1), demonstrating that first-pass metabolism is minimal. Oral absorption of theophylline was rapid, and similar MRT values were obtained after intravenous and oral dosing (Table 1). The total clearance (CL_{total}) of etoposide in monkeys and rats was smaller than the hepatic blood flow (2616 and 2832 mL/h/kg in monkey and rat, respectively)(16)(Table 1). Even when the blood-to-plasma concentration ratio for etoposide (0.7 and 1.0 in monkey and rat, respectively) is taken into consideration, blood clearance was lower than the hepatic blood flow, suggesting that hepatic first-pass extraction is minor (~ 0.05) in monkey and moderate (~ 0.55) in rat, and intestinal availability primarily limits oral bioavailability in both species. Digoxin also showed little hepatic first-pass effect, and the oral bioavailability appears to be determined by the intestinal permeation, since the blood clearance is sufficiently lower than the hepatic blood flow (Table 1). The bioavailability of etoposide and digoxin in monkeys (10~20%, Table 1) is much lower than that in humans (52% and 70%, respectively)(15). One of the possible explanations is that species differences exist in the intestinal permeability of these drugs, although we cannot exclude the other possibility that the formulation of them would affect the oral bioavailability, as suggested by Shah et al. for the absorption of etoposide in rats (17). Although the values of distribution volume ($V_{d(ss)}$) of digoxin and theophylline were similar between monkeys and rats, that of etoposide was lower in monkeys than in rats (Table 1). This may be because of species difference in plasma protein binding (the plasma free fraction of etoposide was estimated to be 0.02 and 0.23 in monkeys and rats, respectively).

Transport of etoposide, digoxin and theophylline across upper, middle and lower small intestine of monkeys and rats

To evaluate the intestinal availability of etoposide in monkeys, the

intestinal permeability of etoposide, digoxin (or [³H]digoxin) and theophylline was measured in an Ussing-type chamber. Permeability of FD-4 (or [¹⁴C]inulin) as a slowly absorbed marker drug was also evaluated. To avoid nonlinear transport and cellular toxicity, the concentration of etoposide or digoxin in the donor-side chamber was set as low as possible, consistent with obtaining a detectable level in the acceptor-side chamber. Since the major intestinal site for the absorption of etoposide was not known, we divided the small intestine into three segments (upper, middle and lower parts). The permeability of each segment in the AP-to-BL and BL-to-AP directions was measured, and transport clearances of each compound were calculated by using Eq(1) and (2), as shown in Fig. 2. No efflux transport of etoposide or digoxin was observed in monkeys, whereas clear efflux ($CL_{sec} > CL_{abs}$) of etoposide and digoxin was observed in all the segments and lower segment of rat small intestine, respectively (Fig. 2), suggesting that the intestinal P-gp function in monkeys is less active than in rats. In contrast to theophylline, the permeability of which was much higher than that of FD-4 in all segments of both monkeys and rats (Fig. 2), the AP-to-BL transport of etoposide or digoxin was close to that of FD-4 in monkeys and rats (Fig. 2). These results indicate that the limited bioavailability of etoposide in monkeys and rats is a consequence of smaller intestinal permeability. In monkeys, the permeability of FD-4 was slightly higher in the lower part than the upper and middle parts (Fig. 2A). Although the reason for this result is unknown, this may be relevant to the similar regional difference for the permeability of etoposide and digoxin (Fig. 2A).

Intestinal absorption mechanism assessed by model analysis

To understand in detail the intestinal absorption mechanism of etoposide, permeability across the apical and basolateral membranes was separately estimated based on the Ussing-type chamber data, assuming a steady-state condition. The parameters obtained are listed in Table 2. Note that not all the data are directly comparable. Comparison between CL_{TA} and CL_{TB} and that between CL_{AT} and CL_{BT} are reasonable since both parameters are intrinsic clearances based on drug concentration in the donor side of chamber, where all the drug molecules are assumed to be in unbound (free) form. On the other hand, CL_{TA} and CL_{TB} shown in the present study represent $f_t \times CL_{TAf}$ and $f_t \times CL_{TBf}$,

respectively, where f_t , CL_{TAf} and CL_{TBf} are the free fraction in tissue, the intrinsic apical efflux clearance from tissue and the intrinsic basal efflux clearance from tissue, respectively. We evaluated CL_{TA} and CL_{TB} instead of CL_{TAf} and CL_{TBf} , since we could not determine f_t for technical reasons. Therefore, direct comparison between CL_{AT} and CL_{TA} is not appropriate. In the case of comparison of membrane permeability between drugs or animal species, direct comparison of CL_{AT} or CL_{BT} is reasonable, but comparison between CL_{TA} or CL_{TB} may not be acceptable since f_t values are variable from compound to compound.

CL_{AT} of etoposide in monkey small intestine was markedly lower than that in rats, whereas CL_{AT} of theophylline was similar in monkeys and rats (Table 2). Regional difference of CL_{AT} of etoposide was at most 2-fold in monkey small intestine, whereas CL_{AT} of etoposide in rat lower small intestine was approximately 6-fold higher than that in the upper small intestine (Table 2). In monkey upper and middle small intestine, CL_{TA} of etoposide was much lower than CL_{TB} , whereas the difference between CL_{TA} and CL_{TB} of theophylline was at most 2-fold (Table 2). Consequently, the CL_{abs} values of etoposide were close to CL_{AT} (Fig. 2, Table 2), indicating that apical uptake of etoposide is the rate-limiting step of intestinal absorption in monkeys. Similar results were also obtained for digoxin, although significant difference between CL_{TA} and CL_{TB} was obtained only in monkey lower intestine. However, in rat small intestine, especially in the lower segment, the values of CL_{TA} of etoposide and digoxin were higher than CL_{TB} , whereas CL_{TA} of theophylline was similar to CL_{TB} (Table 2). These results indicate that once etoposide and digoxin are taken up by intestinal tissues across the apical membrane in rats, they are mostly excreted back into the intestinal lumen, whereas theophylline taken up across the apical membrane is distributed almost equally to the apical and basal membrane sides. The values of CL_{TA} of etoposide and digoxin in rats gradually increased from the upper to the lower small intestine, and this is consistent with the reported regional differences of P-gp function and expression (14, 18).

P-gp expression in monkey and rat small intestines

To assess the P-gp function in monkey small intestine, we measured P-gp expression in monkey and rat small intestines by Western blot analysis.

Specific bands for P-gp was detected at around 170 kDa (Fig. 3). Monkey small intestine exhibited little regional difference, whereas expression in rat lower intestine tended to be higher than that in rat upper one, although there was no statistical significance (Fig. 3).

Discussion

Monkeys tend to exhibit lower oral drug bioavailability than humans (1, 2). Indeed, we observed extensive metabolism of midazolam, a typical substrate of CYP3A, in small intestine of monkeys, and suggested that difference of intestinal metabolism might be the key to the species difference in the oral bioavailability of midazolam (4). However, oral bioavailability is influenced by membrane permeability (e.g., P-gp activity), as well as intracellular metabolism (e.g., CYP3A activity) and other factors (5, 6). In the present study, CL_{total} of etoposide was low and close to that of theophylline, the bioavailability of which is close to unity in monkeys (Table 1), indicating that there is a negligible hepatic first-pass effect in the case of etoposide. Nevertheless, the oral bioavailability of etoposide in monkeys (Table 1) was much lower than that in humans (~52%, 15). Therefore, we hypothesized that intestinal absorption of etoposide in monkeys was less than in humans.

To investigate the intestinal absorption mechanism of etoposide, we utilized an Ussing-type chamber system and measured AP-to-BL and BL-to-AP transport of etoposide, as well as several reference compounds, i.e., digoxin, another P-gp substrate, theophylline, a rapidly absorbed and poorly first-pass-metabolized marker, and FD-4 (or [³H]inulin), a slow absorption marker, in the upper, middle and lower small intestine of monkey and rat. Intestinal permeability (CL_{abs}) of etoposide and digoxin in both species was similar to that of FD-4 (or [³H]inulin), suggesting that the permeability of both compounds would be low (Fig. 2). On the other hand, the extent of oral bioavailability of etoposide and digoxin in rats were 13.9% and 52.8%, respectively (Table 1), being much greater than the fraction absorbed of inulin in rats (~3.5% of dose), as estimated from the urinary excretion of inulin after oral administration (19). These results indicate that it is difficult to predict the *in vivo* fraction absorbed from intestinal permeability data, even if freshly isolated intestinal tissue is available. One of the possible explanations would be the difference in concentration gradient between luminal and blood sides *in vivo* which was not considered in the present study, but may drive greater mass across the intestine, affecting oral bioavailability. In rats, however, CL_{sec} of etoposide and digoxin was higher than CL_{abs} in the lower small intestine (Fig. 2), and this is consistent with findings by other groups (14,

20). Vectorial transport across the small intestine, which is thought to reflect the contribution of efflux transporter(s), is usually evaluated in terms of the efflux ratio (CL_{sec}/CL_{abs}). Values of efflux ratio of etoposide and digoxin in monkey intestine were much lower than that in rat intestine (Fig. 2), suggesting that there is a difference in the contribution of efflux transporter(s) (possibly P-gp) between monkeys and rats.

The Ussing-type chamber system is useful technique to separately estimate microscopic parameters representing permeability across basal and apical membranes. However, this system needs appropriate control studies using both rapid and slow absorption markers (theophylline and FD-4 or inulin, respectively, in the current study). Both FD-4 and inulin are often used as paracellular markers, and the permeability of these compounds could actually include the permeability through the paracellular route. Nevertheless, as shown in Fig. 2, the permeability of FD-4 was higher than that of etoposide and digoxin in monkey duodenum (Fig. 2). This cannot be explained even if we consider that FD-4 is the paracellular marker, and permeability of FD-4 may not adequately represent the paracellular route of etoposide or digoxin. Therefore, those slow absorption markers were used in the current study to simply evaluate experimental technique and variability in Ussing-type chamber studies. On the other hand, permeability of FD-4 or inulin was close to that of etoposide and digoxin with the exception of secretory directions in rat middle and lower intestines (Fig. 2), indicating slow permeation of etoposide and digoxin. However, we measured the amount of etoposide, digoxin and inulin associated with the tissues in rats at the end of the chamber experiments, and the tissue-associated amount of etoposide in monkeys and rats, and that of etoposide in rats were much higher than that of inulin (data not shown), suggesting that etoposide and digoxin could be accumulated inside the tissues other than the paracellular space, and subjected, at least partly, to the transcellular permeation. Therefore, in the present study, we estimated microscopic parameters to compare the membrane permeability with each other (Table 2).

Troutman et al. suggested that efflux ratio is not an appropriate indicator for assessing the influence of P-gp on CL_{abs} (21). In the present study, we quantitatively analyzed the permeability of each intestinal membrane with the

use of a simple kinetic model to understand in more detail the species difference in the intestinal transport (Fig. 4). CL_{TA} of etoposide was much higher than CL_{TB} in rat small intestine, indicating that intestinal absorption of etoposide was limited by P-gp function in rats (Table 2, Fig. 4), which is consistent with previous findings by other groups. On the contrary, apical uptake clearance (CL_{AT}) of etoposide in monkey small intestine was markedly lower than that of theophylline and was close to CL_{abs} (Fig. 2, Table 2), indicating that apical uptake is the rate-limiting process of intestinal etoposide absorption in monkey (Fig. 4). It should also be noted that CL_{abs} of etoposide and digoxin was close to that of FD-4 especially in monkeys (Fig. 2). This indicates smaller membrane permeability in monkeys, compared with rats, but the contribution of paracellular route to the overall intestinal permeability should also be considered.

CL_{AT} of etoposide in rat small intestine was higher than that in monkeys, although CL_{AT} of theophylline was similar in monkeys and rats (Table 2), implying that an active transport system(s) is involved in intestinal uptake of etoposide, at least in rats. This would be consistent with previous reports that the oral AUC of etoposide was saturated with increasing dose, and was decreased by grapefruit juice intake (22-24). Moreover, according to Lipinski's "rule-of-5" or the prediction method based on the value of polar surface area (12, 25, 26), poor absorption of etoposide can be expected owing to its physicochemical characteristics (12). However, etoposide exhibits higher bioavailability in humans (> 50% of dose after oral administration) than in laboratory animals. Therefore, it is possible that species difference of intestinal absorption of etoposide is associated with a transport system(s) that is functionally expressed in humans and rats, but poorly expressed in monkeys. Values of CL_{TA} of etoposide and digoxin in the lower small intestine of monkey and rat were higher than those in the upper segment of the small intestine (Table 2). This is compatible with the regional difference in P-gp expression in rats (Fig. 3), but such a regional difference in P-gp expression was not observed in monkeys (Fig. 3). These results indicate that the regional difference of CL_{TA} cannot be fully explained by P-gp, and another efflux transporter(s) and/or intracellular binding may influence intestinal efflux in monkeys.

We also measured the intestinal permeability of etoposide and digoxin

at higher concentrations (300 μM etoposide and 250 μM digoxin) than 30 μM in rat upper, middle and lower small intestine. In the lower small intestine, CL_{abs} of digoxin examined at 250 μM ($3.35 \pm 0.75 \times 10^{-6}$ cm/sec) was higher than that at 30 μM (Fig. 2), whereas little difference was seen in the case of etoposide. Therefore, P-gp may be more easily saturated with digoxin than with etoposide, i.e., saturation of P-gp favors digoxin absorption in rats. Moreover, it has been suggested that an influx transporter is involved in digoxin absorption (27). Organic anion transporting polypeptide 2 (Oatp2, Slco1a3), which can transport digoxin, is expressed in the small intestine, at least at the mRNA level (28, 29). However, its human ortholog OATP-A (SLCO1A2), which is also expressed in the small intestine, does not transport digoxin (30, 31). In monkeys, on the other hand, we have only measured the intestinal permeability of etoposide and digoxin at 30 μM due to the detection limit. Therefore, we cannot conclude any possible saturation in the influx and/or efflux transport systems in monkeys. Further studies are necessary to clarify all the factors affecting absorption of digoxin and etoposide.

In addition to P-gp, MRP2 (ABCC2) and BCRP (ABCG2) are also expressed on apical membranes of small intestinal epithelial cells (7-9). Although etoposide is a substrate of both of them (32, 33), P-gp mainly regulates its intestinal absorption in mice (13), and this is consistent with our present finding that P-gp is involved in the intestinal absorption of etoposide in rats (Figs. 2, 3). In contrast to rodents, monkeys showed little involvement of P-gp in intestinal permeation of etoposide or digoxin (Fig. 2, Table 2), although P-gp expression was detected in all segments of the small intestine (Fig. 3), and the P-gp-mediated etoposide transport seemed to be larger in monkey than in rat (efflux ratios: 3.3 in monkey MDR1-expressing pcLLC.1 cells and 1.6 in rat Mdr1a-expressing pcLLC.1 cells) (34). One possibility would be the functional difference in the transport of etoposide and digoxin between the two species form of P-gp endogenously expressed in small intestine. Another possibility is that rapid basolateral efflux might mask the apical efflux mediated by P-gp. Indeed, the basolateral efflux (CL_{TB}) of etoposide and digoxin was greater than the apical efflux (CL_{TA}) in monkey intestine (Table 2). Therefore, it is possible that a transport system(s) is involved in basolateral efflux of etoposide and

digoxin in monkeys. MRP3 (ABCC3), which transports etoposide, is localized on the basolateral membrane (35). Further, it was reported that etoposide is an inhibitor of monkey MRP1, but a good substrate for human MRP1, and a poor substrate for murine Mrp1 (36). Accordingly, these MRPs are candidate transporters responsible for basolateral efflux of etoposide in monkey, and it will be necessary to investigate the expression and function of MRPs in monkey small intestine.

In conclusion, we have demonstrated limited intestinal availability of etoposide and digoxin in both monkeys and rats. Kinetic analysis revealed that intestinal absorption of etoposide and digoxin is limited by apical uptake in monkeys, whereas back efflux to the luminal side mediated by P-gp limits the intestinal absorption in rats, but not in monkeys. Although the oral bioavailability of etoposide is similarly suppressed by limited intestinal permeability in both rats and monkeys, the intestinal absorption mechanism is thus different between the two species. Species difference of oral bioavailability between humans and these animals is likely to be caused by a difference in intestinal permeability.

References

1. K. W. Ward, R. Nagilla, and L. J. Jolivet. Comparative evaluation of oral systemic exposure of 56 xenobiotics in rat, dog, monkey and human. *Xenobiotica* **35**: 191-210 (2005).
2. W. L. Chiou and P. W. Buehler. Comparison of oral absorption and bioavailability of drugs between monkey and human. *Pharm Res* **19**: 868-74 (2002).
3. W. K. Sietsema. The absolute oral bioavailability of selected drugs. *Int J Clin Pharmacol Ther Toxicol* **27**: 179-211 (1989).
4. T. Nishimura, N. Amano, Y. Kubo, M. Ono, Y. Kato, H. Fujita, Y. Kimura, and A. Tsuji. Asymmetric intestinal first-pass metabolism causes minimal oral bioavailability of midazolam in cynomolgus monkey. *Drug Metab Dispos* **35**: 1275-84 (2007).
5. P. B. Watkins. The barrier function of CYP3A4 and P-glycoprotein in the small bowel. *Adv Drug Deliv Rev* **27**: 161-170 (1997).
6. L. Z. Benet, C. L. Cummins, and C. Y. Wu. Unmasking the dynamic interplay between efflux transporters and metabolic enzymes. *Int J Pharm* **277**: 3-9 (2004).
7. M. Maliepaard, G. L. Scheffer, I. F. Faneyte, M. A. van Gastelen, A. C. Pijnenborg, A. H. Schinkel, M. J. van De Vijver, R. J. Scheper, and J. H. Schellens. Subcellular localization and distribution of the breast cancer resistance protein transporter in normal human tissues. *Cancer Res* **61**: 3458-64 (2001).
8. A. D. Mottino, T. Hoffman, L. Jennes, and M. Vore. Expression and localization of multidrug resistant protein mrp2 in rat small intestine. *J Pharmacol Exp Ther* **293**: 717-23 (2000).
9. M. F. Fromm, H. M. Kauffmann, P. Fritz, O. Burk, H. K. Kroemer, R. W. Warzok, M. Eichelbaum, W. Siegmund, and D. Schrenk. The effect of rifampin treatment on intestinal expression of human MRP transporters. *Am J Pathol* **157**: 1575-80 (2000).
10. Q. Wang, R. K. Bhardwaj, D. Herrera-Ruiz, N. N. Hanna, I. T. Hanna, O. S.

- Gudmundsson, T. Buranachokpaisan, I. J. Hidalgo, and G. T. Knipp. Expression of multiple drug resistance conferring proteins in normal Chinese and Caucasian small and large intestinal tissue samples. *Mol Pharm* **1**: 447-54 (2004).
11. T. Terao, E. Hisanaga, Y. Sai, I. Tamai, and A. Tsuji. Active secretion of drugs from the small intestinal epithelium in rats by P-glycoprotein functioning as an absorption barrier. *J Pharm Pharmacol* **48**: 1083-9 (1996).
 12. M. Takano, R. Yumoto, and T. Murakami. Expression and function of efflux drug transporters in the intestine. *Pharmacol Ther* **109**: 137-61 (2006).
 13. J. D. Allen, S. C. Van Dort, M. Buitelaar, O. van Tellingen, and A. H. Schinkel. Mouse breast cancer resistance protein (Bcrp1/Abcg2) mediates etoposide resistance and transport, but etoposide oral availability is limited primarily by P-glycoprotein. *Cancer Res* **63**: 1339-44 (2003).
 14. V. D. Makhey, A. Guo, D. A. Norris, P. Hu, J. Yan, and P. J. Sinko. Characterization of the regional intestinal kinetics of drug efflux in rat and human intestine and in Caco-2 cells. *Pharm Res* **15**: 1160-7 (1998).
 15. J. G. Hardman and L. E. Limbird. *Goodman & Gilman's: The Pharmacological Basis of Therapeutics*, McGraw-Hill Companies, Inc., New York, 2001.
 16. B. Davies and T. Morris. Physiological parameters in laboratory animals and humans. *Pharm Res* **10**: 1093-5 (1993).
 17. J. C. Shah, J. R. Chen, and D. Chow. Oral bioavailability and in situ absorption of etoposide in rat. *Int J Pharm* **84**: 223-32 (1992).
 18. R. Tian, N. Koyabu, H. Takanaga, H. Matsuo, H. Ohtani, and Y. Sawada. Effects of grapefruit juice and orange juice on the intestinal efflux of P-glycoprotein substrates. *Pharm Res* **19**: 802-9 (2002).
 19. A. V. Kamath, R. A. Morrison, T. W. Harper, S. J. Lan, A. M. Marino, and S. Chong. Multiple pathways are involved in the oral absorption of BMS-262084, a tryptase inhibitor, in rats: role of paracellular transport, binding to trypsin, and P-glycoprotein efflux. *J Pharm Sci* **94**: 1115-23

- (2005).
20. R. H. Stephens, J. Talianis-Hughes, N. B. Higgs, M. Humphrey, and G. Warhurst. Region-dependent modulation of intestinal permeability by drug efflux transporters: in vitro studies in *mdr1a(-/-)* mouse intestine. *J Pharmacol Exp Ther* **303**: 1095-101 (2002).
 21. M. D. Troutman and D. R. Thakker. Efflux ratio cannot assess P-glycoprotein-mediated attenuation of absorptive transport: asymmetric effect of P-glycoprotein on absorptive and secretory transport across Caco-2 cell monolayers. *Pharm Res* **20**: 1200-9 (2003).
 22. V. J. Harvey, M. L. Slevin, S. P. Joel, A. Johnston, and P. F. Wrigley. The effect of dose on the bioavailability of oral etoposide. *Cancer Chemother Pharmacol* **16**: 178-81 (1986).
 23. S. Reif, M. C. Nicolson, D. Bisset, M. Reid, C. Kloft, U. Jaehde, and H. L. McLeod. Effect of grapefruit juice intake on etoposide bioavailability. *Eur J Clin Pharmacol* **58**: 491-4 (2002).
 24. K. R. Hande, M. G. Krozely, F. A. Greco, J. D. Hainsworth, and D. H. Johnson. Bioavailability of low-dose oral etoposide. *J Clin Oncol* **11**: 374-7 (1993).
 25. D. E. Clark. Rapid calculation of polar molecular surface area and its application to the prediction of transport phenomena. 1. Prediction of intestinal absorption. *J Pharm Sci* **88**: 807-14 (1999).
 26. C. A. Lipinski, F. Lombardo, B. W. Dominy, and P. J. Feeney. Experimental and computational approaches to estimate solubility and permeability in drug discovery and development settings. *Adv Drug Deliv Rev* **46**: 3-26 (2001).
 27. H. M. Yao and W. L. Chiou. The complexity of intestinal absorption and exsorption of digoxin in rats. *Int J Pharm* (2006).
 28. B. Noe, B. Hagenbuch, B. Stieger, and P. J. Meier. Isolation of a multispecific organic anion and cardiac glycoside transporter from rat brain. *Proc Natl Acad Sci U S A* **94**: 10346-50 (1997).
 29. X. Cheng, J. Maher, C. Chen, and C. D. Klaassen. Tissue distribution and ontogeny of mouse organic anion transporting polypeptides (Oatps). *Drug Metab Dispos* **33**: 1062-73 (2005).

30. G. A. Kullak-Ublick, M. G. Ismail, B. Stieger, L. Landmann, R. Huber, F. Pizzagalli, K. Fattinger, P. J. Meier, and B. Hagenbuch. Organic anion-transporting polypeptide B (OATP-B) and its functional comparison with three other OATPs of human liver. *Gastroenterology* **120**: 525-33 (2001).
31. Y. Su, X. Zhang, and P. J. Sinko. Human organic anion-transporting polypeptide OATP-A (SLC21A3) acts in concert with P-glycoprotein and multidrug resistance protein 2 in the vectorial transport of Saquinavir in Hep G2 cells. *Mol Pharm* **1**: 49-56 (2004).
32. R. H. Stephens, C. A. O'Neill, J. Bennett, M. Humphrey, B. Henry, M. Rowland, and G. Warhurst. Resolution of P-glycoprotein and non-P-glycoprotein effects on drug permeability using intestinal tissues from *mdr1a (-/-)* mice. *Br J Pharmacol* **135**: 2038-46 (2002).
33. A. Guo, W. Marinaro, P. Hu, and P. J. Sinko. Delineating the contribution of secretory transporters in the efflux of etoposide using Madin-Darby canine kidney (MDCK) cells overexpressing P-glycoprotein (Pgp), multidrug resistance-associated protein (MRP1), and canalicular multispecific organic anion transporter (cMOAT). *Drug Metab Dispos* **30**: 457-63 (2002).
34. T. Takeuchi, S. Yoshitomi, T. Higuchi, K. Ikemoto, S. Niwa, T. Ebihara, M. Katoh, T. Yokoi, and S. Asahi. Establishment and Characterization of the Transformants Stably-Expressing MDR1 Derived from Various Animal Species in LLC-PK(1). *Pharm Res* **23**: 1460-72 (2006).
35. N. Zelcer, T. Saeki, G. Reid, J. H. Beijnen, and P. Borst. Characterization of drug transport by the human multidrug resistance protein 3 (ABCC3). *J Biol Chem* **276**: 46400-7 (2001).
36. B. D. Stride, C. E. Grant, D. W. Loe, D. R. Hipfner, S. P. Cole, and R. G. Deeley. Pharmacological characterization of the murine and human orthologs of multidrug-resistance protein in transfected human embryonic kidney cells. *Mol Pharmacol* **52**: 344-53 (1997).

Legends

Figure 1.

Plasma concentration profiles of etoposide, digoxin and theophylline in monkeys (A, B, C) and rats (D, E, F). Etoposide (A, D), digoxin (B, E) and theophylline (C, F) were intravenously (0.1 mg/kg, ○) and orally (1.0 mg/kg, ●) administered to monkeys and rats. Plasma concentration of each drug was analyzed by LC/MS/MS. Each point represents the mean ± S.D. of three determinations, except for digoxin administration to monkeys (n = 2). Pharmacokinetic parameters are listed in Table 1.

Figure 2. Intestinal permeability of test compounds in monkeys (A) and rats (B). Permeability of etoposide (●), digoxin (or [³H]digoxin for rats) (■), theophylline (◆), FD-4 (◇) and inulin (○) in the upper, middle and lower small intestine was measured in an Ussing-type chamber. Etoposide and digoxin concentration in the donor side of the chamber was set at 30 μM. Theophylline concentration in the donor side of the chamber was set at 300 μM. FD-4 (or [¹⁴C]inulin in the [³H]digoxin transport study) concentration was 100 μM. Data are the mean ± S.E.M. of 3 - 4 determinations. CL_{abs} and CL_{sec} were obtained by dividing the amount of drugs that appeared in acceptor-side chamber by the area under the concentration curve in the donor-side chamber. e, i, d: Significant difference from CL_{abs} for etoposide, inulin and digoxin, respectively ($p < 0.05$).

Figure 3. Western blot analysis of intestinal P-gp in monkeys (A) and rats (B). Membrane proteins (20 μg/lane) prepared from upper, middle and lower small intestine were subjected to 10% SDS-PAGE. Relative band densities (% of upper small intestine) are shown in the lower panel. Each column is the mean ± S.E.M. of 3 - 4 animals.

Figure 4. Schematic illustration of intestinal absorption mechanism for etoposide in monkey and rat. CL_{AT} , CL_{TA} , CL_{TB} and CL_{BT} mean membrane permeability (see text). The kinetic model shown represents that for all the segments of small intestine, but the higher permeability across the apical membranes (CL_{AT} and CL_{TA}) in rats is more obvious in the lower part of small intestine.

Table 1. Pharmacokinetic parameters for etoposide, digoxin and theophylline in monkeys and rats^{a)}

Monkey	Etoposide		Digoxin		Theophylline	
	0.1 mg/kg (iv)	1 mg/kg (oral)	0.1 mg/kg (iv)	1 mg/kg (oral)	0.1 mg/kg (iv)	1 mg/kg (oral)
C_{max} (ng/mL)	–	137 ± 27	–	8.8	–	794 ± 75
T_{max} (hr)	–	1.67 ± 0.58	–	0.75	–	6.67 ± 2.31
AUC_{0-last} (ng·hr/mL)	1138 ± 233	1490 ± 427	260	158	1539 ± 44	14594 ± 796
CL_{total} (mL/hr/kg)	90 ± 19	–	397	–	65 ± 2	–
V_{dss} (mL/kg)	164 ± 19	–	3519	–	577 ± 9	–
MRT (hr)	1.84 ± 0.18	6.10 ± 0.10	8.97	11.36	8.88 ± 0.31	10.26 ± 0.71
F (%)	–	12.9 ± 1.8	–	21.2	–	94.9 ± 6.2
MAT (hr)	–	4.26 ± 0.21	–	2.43	–	1.38 ± 0.77

Rat	Etoposide		Digoxin		Theophylline	
	0.1 mg/kg (iv)	1 mg/kg (oral)	0.1 mg/kg (iv)	1 mg/kg (oral)	0.1 mg/kg (iv)	1 mg/kg (oral)
C_{max} (ng/mL)	–	22.0 ± 0.5	–	58.4 ± 8.4	–	898 ± 168
T_{max} (hr)	–	0.75 ± 0.43	–	2.67 ± 1.15	–	1.00 ± 0.00
AUC_{0-last} (ng·hr/mL)	65.2 ± 6.2	90.4 ± 36.5	86.4 ± 13.2	457 ± 85	884 ± 63	7621 ± 1914
CL_{total} (mL/hr/kg)	1542 ± 138	–	1177 ± 195	–	114 ± 8	–
V_{dss} (mL/kg)	849 ± 36	–	2722 ± 460	–	506 ± 24	–
MRT (hr)	0.55 ± 0.06	2.65 ± 0.94	2.31 ± 0.12	4.79 ± 0.78	4.45 ± 0.13	4.98 ± 0.21
F (%)	–	13.9 ± 5.8	–	52.8 ± 12.8	–	86.2 ± 22.5
MAT (hr)	–	2.1 ± 0.94	–	2.48 ± 0.79	–	0.53 ± 0.25

a) Each value represents the mean ± S.D. of 3 determinations, except for digoxin in monkey (n = 2).

Table 2. Microscopic parameters representing membrane permeabilities of etoposide, digoxin, and theophylline in monkey and rat

Animal	Test	Segment of small	Concn. ^{b)} (μM)	$\text{CL}_{\text{AT}}^{\text{c)}$ (10^{-6} cm/sec)	$\text{CL}_{\text{TA}}^{\text{d)}$ (10^{-6} cm/sec)	$\text{CL}_{\text{TB}}^{\text{e)}$ (10^{-6} cm/sec)	$\text{CL}_{\text{BT}}^{\text{f)}$ (10^{-6} cm/sec)
Monkey	Etoposide	Upper	30	0.373 ± 0.091	0.180 ^h ± 0.044	2.77 ± 0.54	1.46 ± 0.25
		Middle	30	0.219 ^g ± 0.098	0.080 ^h ± 0.080	1.26 ± 0.41	0.550 ± 0.213
		Lower	30	0.670 ^g ± 0.118	1.62 ± 0.68	2.01 ± 0.08	1.98 ± 0.64
	Digoxin	Upper	30	0.181 ^g ± 0.085	0.342 ± 0.276	1.06 ± 0.43	0.404 ± 0.170
		Middle	30	0.363 ^g ± 0.157	0.198 ± 0.105	1.80 ± 0.95	0.505 ± 0.333
		Lower	30	0.873 ^g ± 0.136	1.59 ^h ± 0.38	3.92 ± 0.30	1.68 ± 0.19
	Theophylline	Upper	300	16.6 ± 2.5	17.8 ± 0.8	37.6 ± 12.2	31.2 ± 7.7
		Middle	300	11.1 ^g ± 0.7	11.9 ^h ± 2.5	21.9 ± 2.6	15.9 ± 2.7
		Lower	300	28.9 ± 6.1	32.9 ± 7.8	32.3 ± 6.1	25.9 ± 5.8
Rat	Etoposide	Upper	30	1.87 ± 0.59	6.37 ± 2.94	3.82 ± 0.33	2.30 ± 0.72
		Middle	30	7.83 ± 1.52	26.9 ^h ± 6.0	5.09 ± 1.15	6.68 ± 0.70
		Lower	30	11.7 ± 2.5	44.2 ^h ± 12.8	6.97 ± 2.50	9.56 ± 1.80
	Digoxin	Upper	30	3.65 ± 0.49	41.1 ± 4.5	36.0 ± 5.7	4.84 ± 0.78
		Middle	30	4.58 ± 0.82	43.2 ± 9.8	38.4 ± 7.2	6.46 ± 1.20
		Lower	30	9.64 ± 1.32	131 ^h ± 26	34.4 ± 3.7	9.02 ± 0.97
	Theophylline	Upper	300	20.7 ± 2.1	58.2 ± 4.6	53.2 ± 1.7	15.1 ± 1.6
		Middle	300	30.8 ± 5.6	90.4 ± 30.5	113 ± 25	24.2 ± 5.8
		Lower	300	45.3 ± 6.2	167 ± 33	154 ± 10	33.5 ± 4.9

a) Each value represents the mean ± S.E.M. of 3-4 determinations.

b) Concentration of the test compound in the donor-side chamber.

c) Membrane permeability across apical membrane from Apical-side buffer into Tissue (AT)

d) Membrane permeability across apical membrane from Tissue into Apical-side buffer (TA)

e) Membrane permeability across basal membrane from Tissue into Basal-side buffer (TB)

f) Membrane permeability across basal membrane from Basal-side buffer into Tissue (BT)

g) Significantly different ($p < 0.05$) from the corresponding values obtained in rats by students' t-test.

h) Significantly different ($p < 0.05$) from CL_{TB} of the same compound, same segments and same species by students' t-test.

Fig. 1

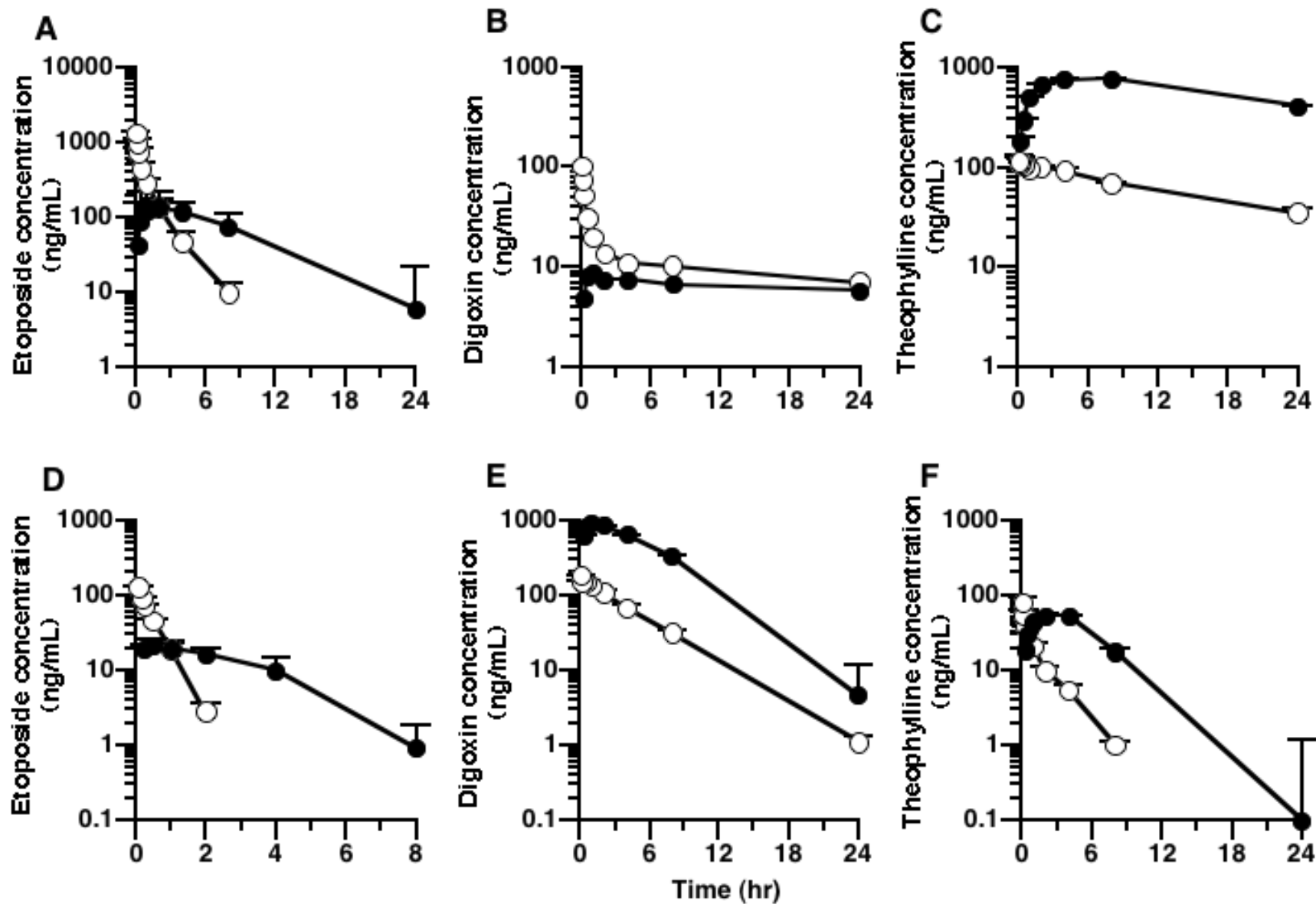


Figure 2

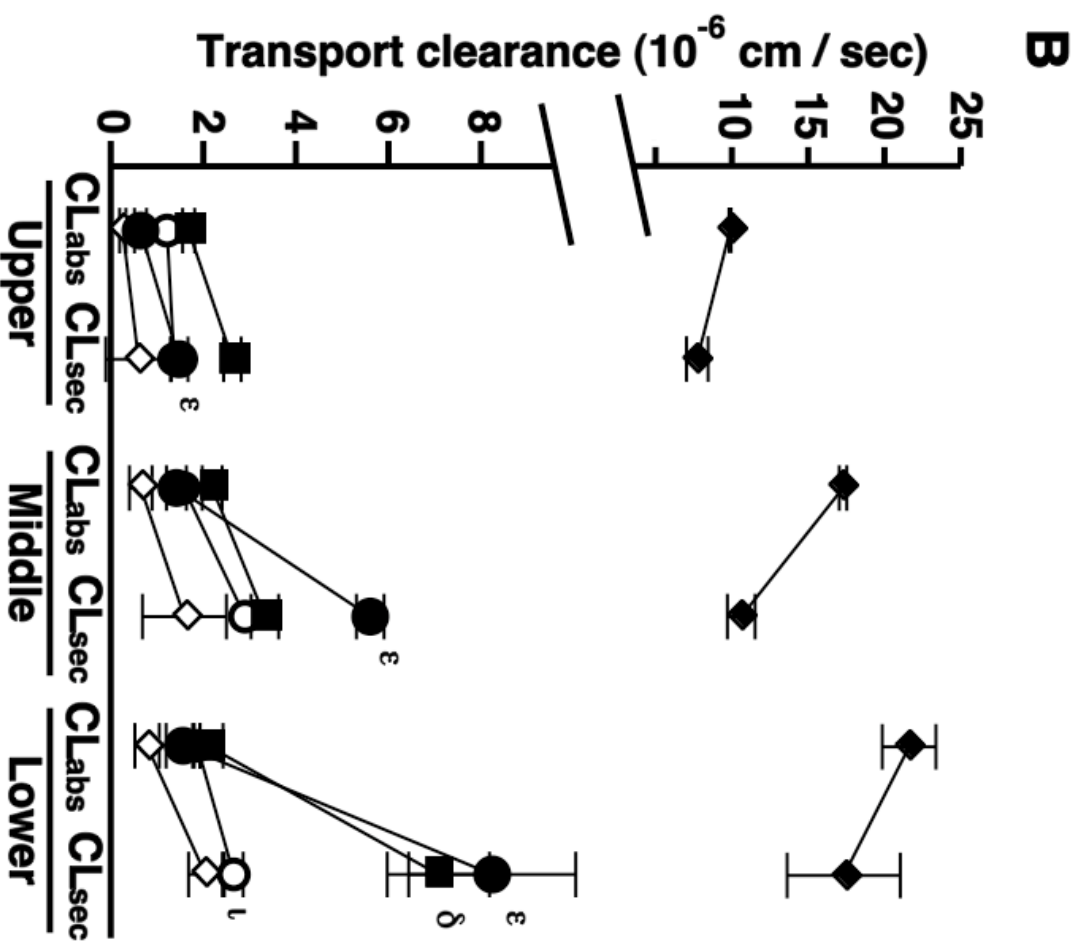
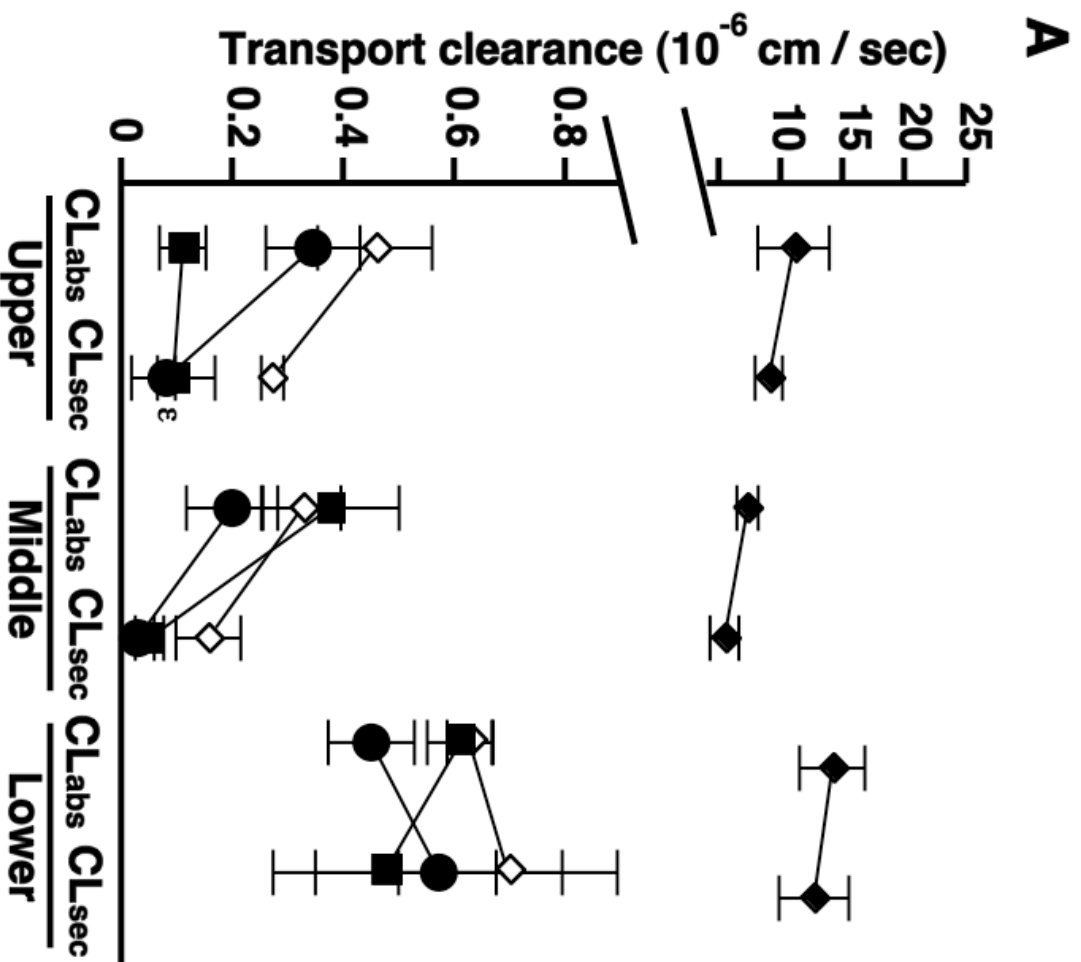
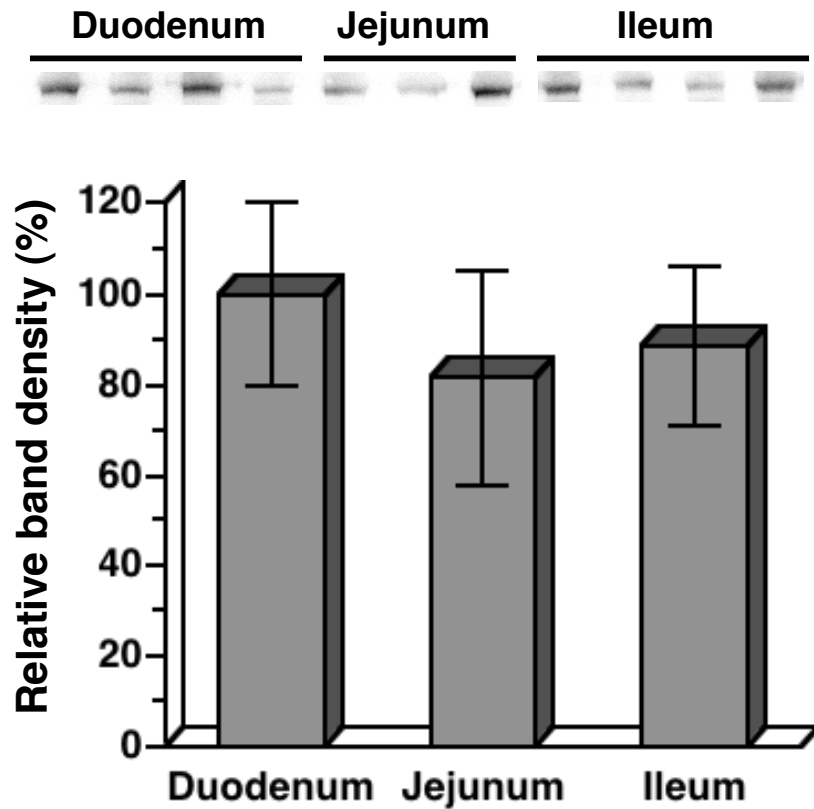


Fig. 3

A



B

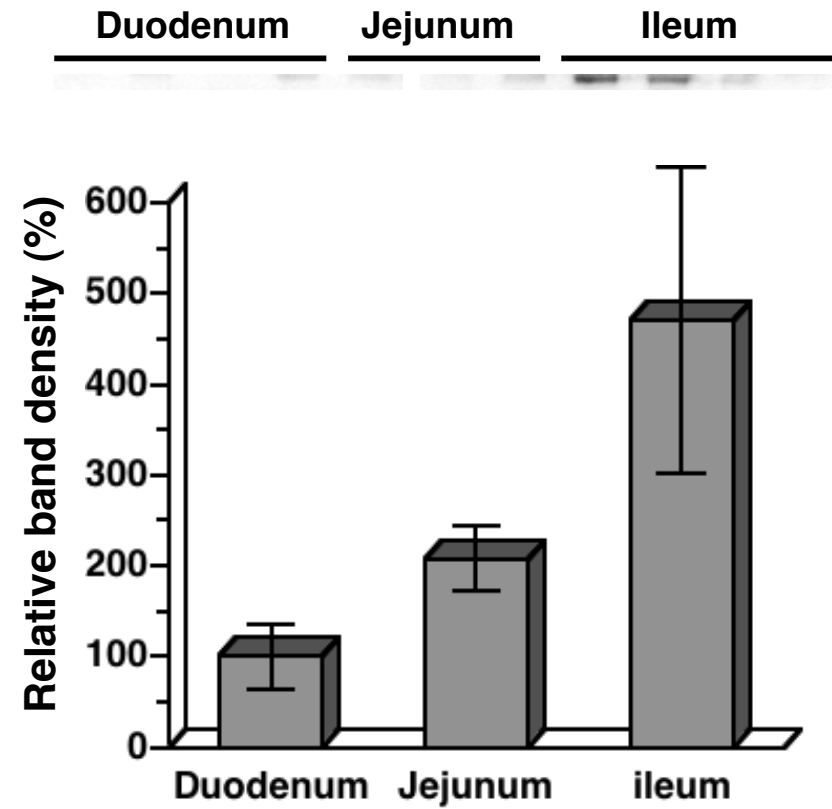
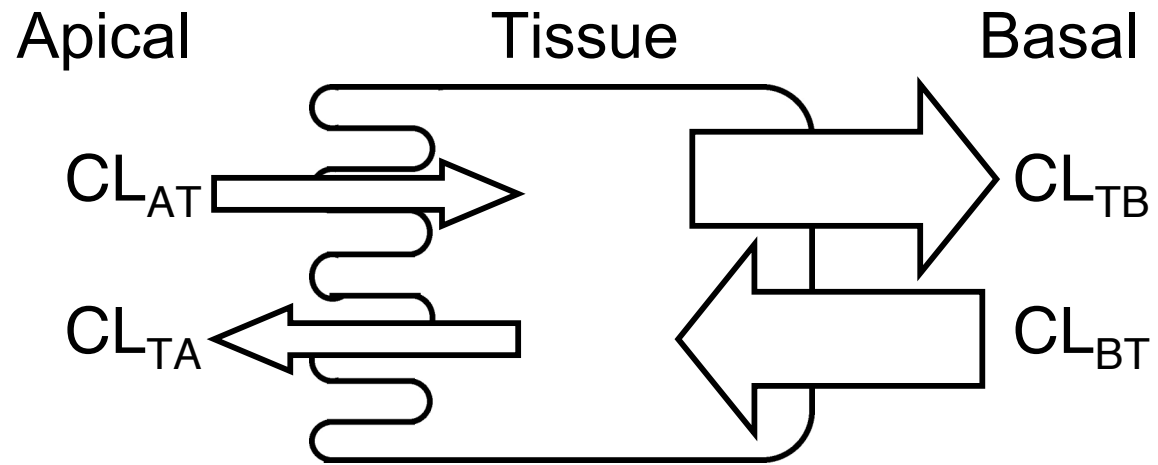


Fig. 4

A Monkey



B Rat

